Supporting information

Ruthenium(II) and Palladium(II) Homo- and Heterobimetallic Complexes: Synthesis, Crystal Structures, Theoretical Calculations and Biological Studies

Banafshe Askari[a], Hadi Amiri Rudbari[a,*], Nicola Micale[b,*], Tanja Schirmeister[c], Thomas Efferth[d], Ean-Jeong Seo[d], Giuseppe Bruno[b], Kevin Schwickert[c]

[a] *Department of Chemistry, University of Isfahan, Isfahan 81746-73441, Iran.*

[b] *Department of Chemical, Biological, Pharmaceutical and Environmental Sciences, University of Messina, Viale Ferdinando Stagno D'Alcontres 31, I-98166 Messina, Italy.*

[c] *Institute of Pharmacy and Biochemistry, Johannes Gutenberg-University, Staudingerweg 5, 55128 Mainz, Germany.*

[d] *Department of Pharmaceutical Biology, Institute of Pharmacy and Biochemistry, Johannes Gutenberg-University, Staudingerweg 5, 55128 Mainz, Germany.*

***** Corresponding authors.

E-mail addresses: h.a.rudbari@sci.ui.ac.ir, hamiri1358@gmail.com (H. Amiri Rudbari), nmicale@unime.it (N. Micale)

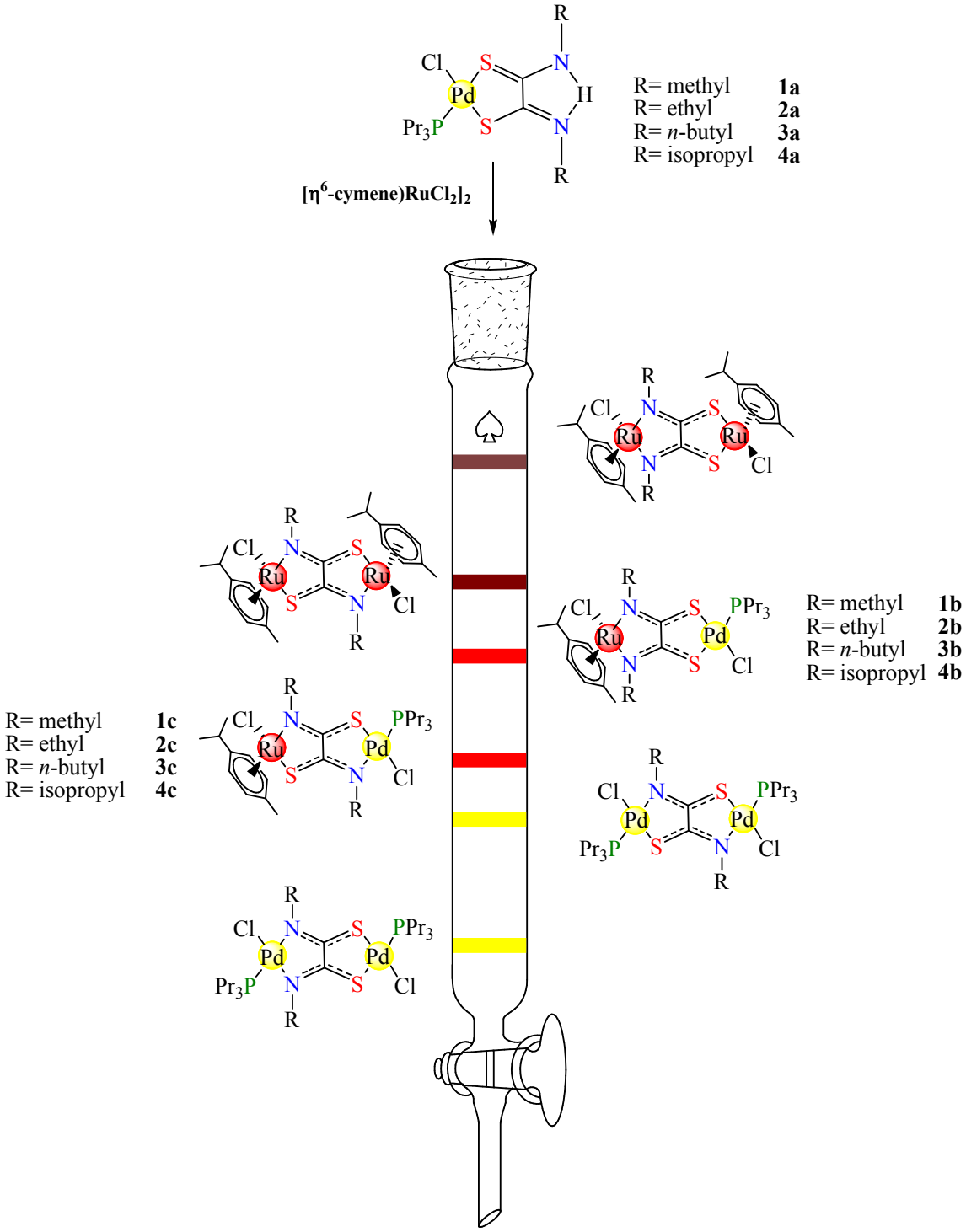

Scheme S1. Route for synthesis of homo- and heterobimetallic complexes in two different coordination modes.

Hirshfeld surface analysis

Hirshfeld surface (HS) analysis (including fingerprint plot) used for a better understanding of the interactions involved in the crystal packing. When Hirshfeld surfaces were proposed as an e□ective way to discern intermolecular interactions in the solid state, the first properties to be mapped on this surface were d_e and d_i, the distances of an atom external or internal to the generated Hirshfeld surface. Combining these two values results in a (d_i, d_e) pair, and binning these into intervals of 0.01 Å (essentially a pixel on the Hirshfeld surface) results in the generation of a fingerprint plot, where the di□erent colors on the fingerprint plot represent the frequency of occurrence of the interaction, increasing from blue to green to red. Taking these (d_i, d_e) pairs and normalizing them with respect to the van der Waals radii of their corresponding atoms results in the d_{norm} surface, with contacts shorter than the sum of the van der Waals radii of the two atoms resulting in a negative value and being highlighted on the d_{norm} surface in red. Contacts close in length to the van der Waals limit are colored white, and blue represents longer contacts.

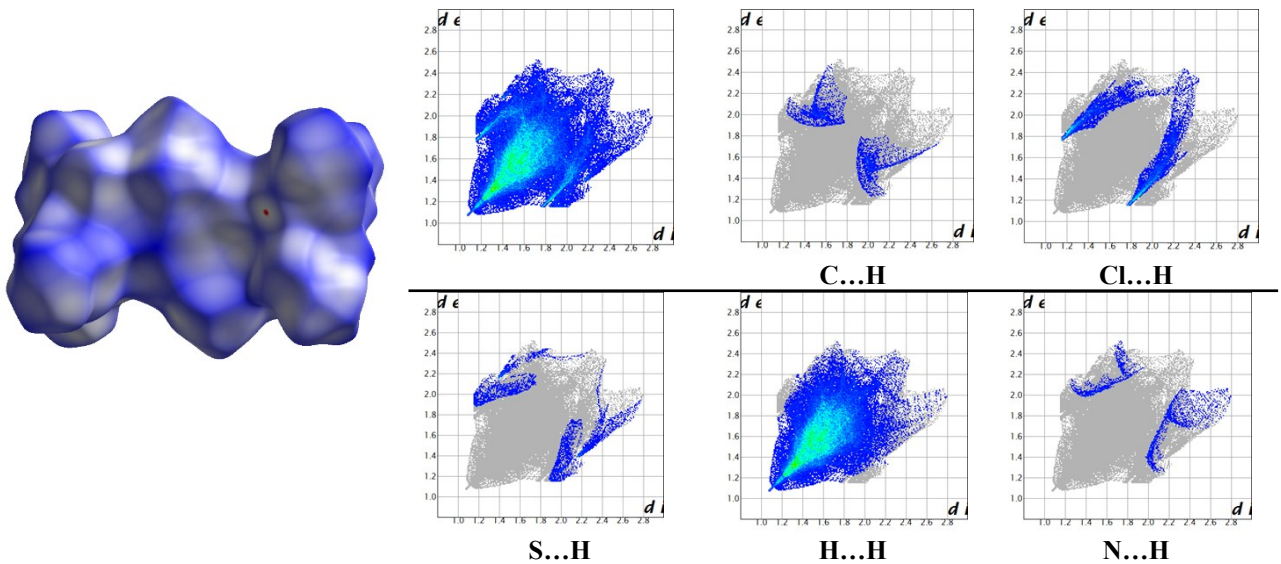

Fig. S1. The Hirshfeld surface graphical representation (d_{norm}) and Hirshfeld surface two-dimensional fingerprint plots for complex **2**. The surface regions with strongest intermolecular interactions in Hirshfeld surface graphical representation are drawn in magenta colour. The d_e

(y axis) and d_i (x axis) values are the closest external and internal distances (Å) from given points on the Hirshfeld surface contacts.

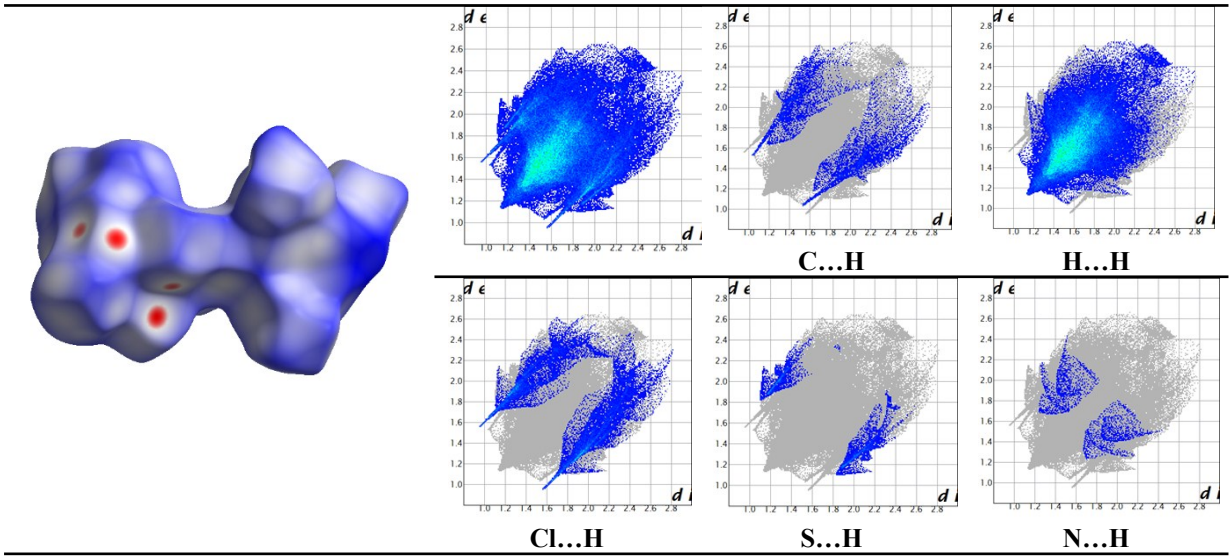

Fig. S2. The Hirshfeld surface graphical representation (d_{norm}) and Hirshfeld surface two-dimensional fingerprint plots for the asymmetric unit of **1c**. The surface regions with strongest intermolecular interactions in Hirshfeld surface graphical representation are drawn in magenta colour. The d_e (y axis) and d_i (x axis) values are the closest external and internal distances (Å) from given points on the Hirshfeld surface contacts.

Hirshfeld surfaces and their associated finger print plots for complexes **2** and **1c** were calculated using CrystalExplorer 17.5 and are illustrated in Figs. S1 and S2. Figure S3 summarize percent of various types of interactions in complexes **2** and **1c**. FPs indicates that most of the contributions over the Hirshfeld surface are due to H…H contact (82.5 and 72.9 % for complexes **2** and **1c**, respectively) as the molecular surface is comprised of a sea of H atoms. As shown in Fig. S3, the H…H interactions appear as the largest region of the fingerprint plot with a high concentration in the middle region, shown in light green. The shortest H…H interaction in the fingerprint plots are presented as sharp spikes at $d_e + d_i = 2.2$ Å.

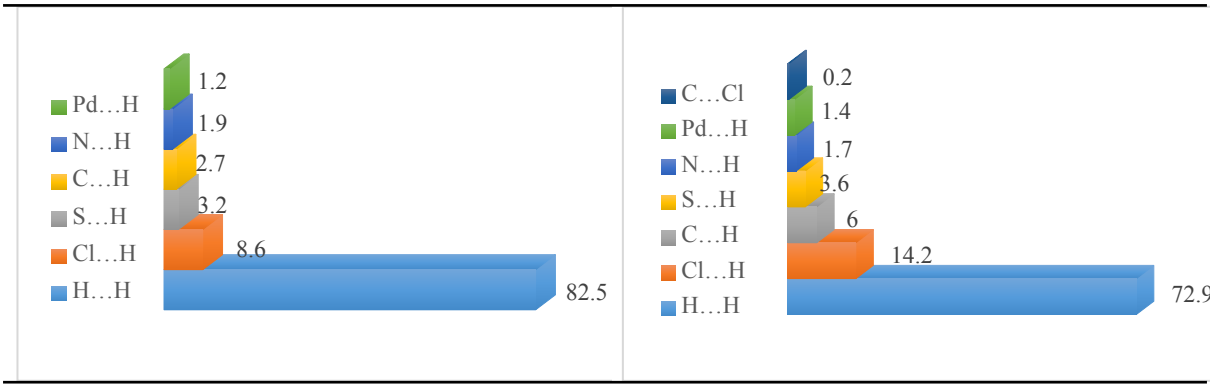

Fig. S3. Relative contributions to the Hirshfeld surface area for intermolecular contacts in complexes **2** (Left) and **1c** (Right).

Large number of H-atoms over surface supported the S...H, C...H, N…H and Pd...H contacts having 3.9, 2.7, 1.9 and 1.2% contributions in complex **2**, respectively. In complex **1c**, S...H, C...H, N…H and Pd...H contacts having 3.6, 6.0, 1.7 and 1.4% contributions, respectively. Also, the decomposition of the fingerprint plots indicates that chlorine intermolecular contacts (Cl...H) cover near to 9% and more than 14% of Hirshfeld surface in complexes **2** and **1c**, respectively. It may be caused by relatively large van der Waals radii of chlorine atom (Fig. S3). Also, this is notable that the Cl...H intermolecular interaction contribution in complex **1c** (14.2 %) is near to twice of Cl...H (8.6 %) in complex **2**. Interestingly, the Cl…H contact distances in **1c** (Cl1…H6B = 2.788 Å and Cl2…H18A = 2.633 Å) is significantly shorter than the corresponding sum of van der Walls radii indicating its prominent role in crystal packing. It seems that this Cl…H short interactions is responsible for zigzag arrangement in crystal packing of complex **1c** (Fig. S4).

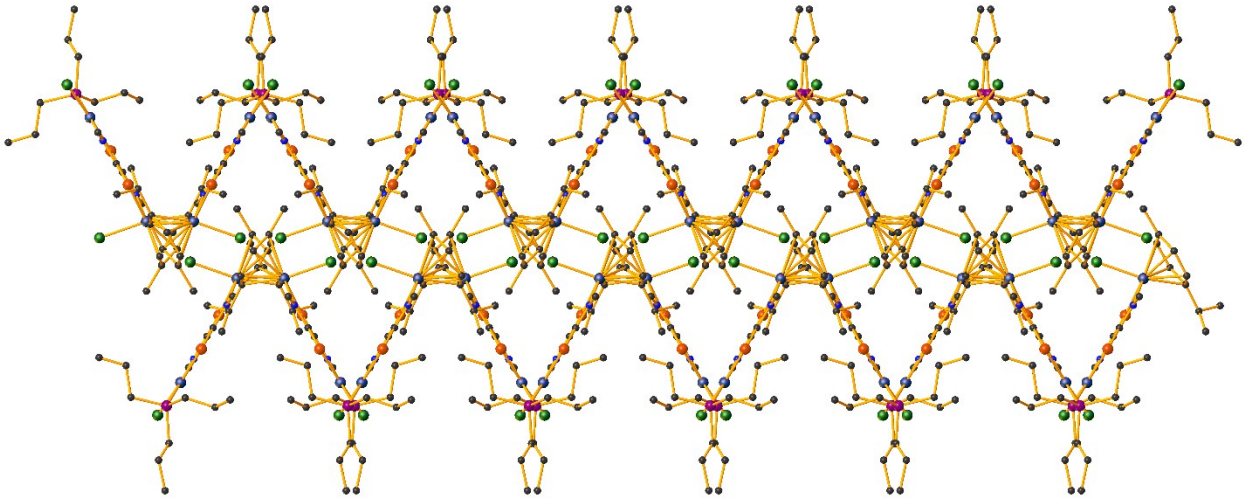

Fig. S4. Crystal packing of **1c** along the c-axis. Hydrogen atoms have been emitted for clarity.

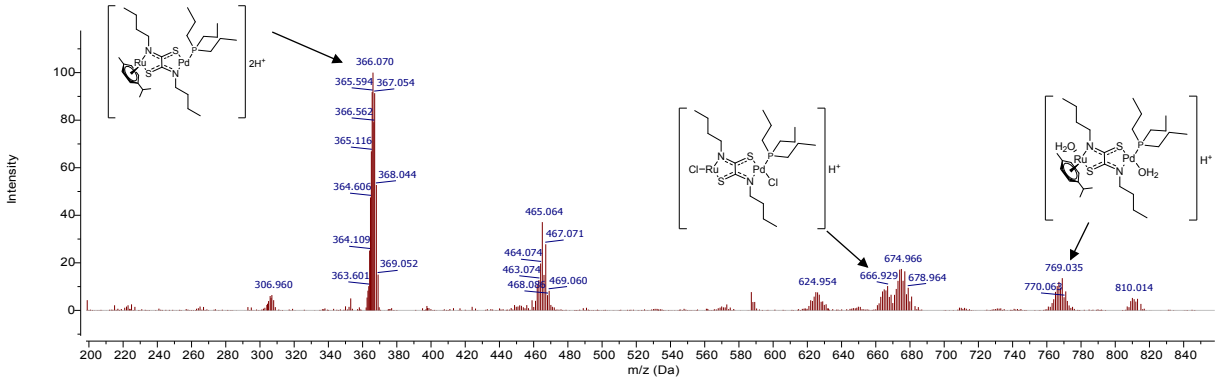

Fig. S5: Mass spectrum of a 10 µM solution of **3c** in 50 mM TRIS-buffer (pH 7.5, 0.03% SDS) after 24 h.

Table S1. E(a.u), selected calculated bond distances (Å) and angles (°) for compounds A, B, C and D; all functionals was used with SDD Basis Set and AUTO fitting set.

Compound A

Functional	PSSTPSS	HSEH1PBE	CAMBLYP	PBE1PBE	ΔE(mean)
E(a.u.)	-3291.846896	-3289.704153	-3290.803390	-3289.541016	
ΔE(HOMO-LUMO)eV	1.86	2.89	5.89	3.65	3.57
Pd(1)-N(1)	2.0595	2.0520	2.0536	2.0487	
Pd(1)-N(2)	2.0471	2.0421	2.0462	2.0384	
Pd(1)-P(1)	2.4041	2.3774	2.3877	2.3739	
Pd(1)-Cl(1)	2.3903	2.3679	2.3677	2.3635	
Ru(1)-S(1)	2.4293	2.4041	2.4167	2.3986	
Ru(1)-S(2)	2.4312	2.4087	2.4222	2.4027	
Ru(1)-Cl(2)	2.4556	2.4340	2.4400	2.4283	
S(1)-C(1)	1.7767	1.7586	1.7572	1.7575	
S(2)-C(2)	1.7746	1.7551	1.7519	1.7538	
N(1)-C(1)	1.3343	1.3168	1.3120	1.3165	
N(2)-C(2)	1.3417	1.3247	1.3201	1.3244	
C(1)-C(2)	1.4802	1.4789	1.4899	1.4789	
N(1)-Pd(1)-P(1)	177.83	177.80	176.68	177.69	
P(1)-Pd(1)-N(2)	100.33	99.80	99.42	99.79	
N(2)-Pd(1)-Cl(1	172.10	172.55	172.76	172.61	
P(1)-Pd(1)-Cl(1)	86.71	87.06	87.37	87.00	
S(2)-Ru(1)-S(1)	85.04	85.20	85.16	85.33	
S(2)-Ru(1)-Cl(2	85.97	86.19	86.71	86.14	
S(1)-Ru(1)-Cl(2)	85.96	86.36	86.87	86.28	

Compound B

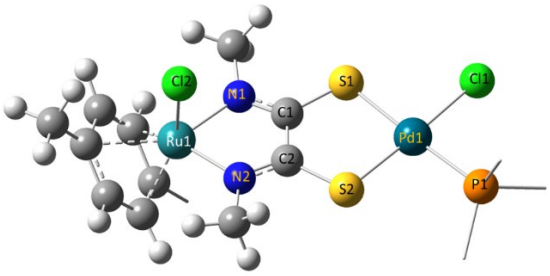

Functional	PSSTPSS	HSEH1PBE	CAMBLYP	PBE1PBE	ΔE(mean)
E(a.u.)	-3291.858549	-3289.718813	-3290.819651	-3289.555637	
ΔE(HO-LU)eV	1.89	3.04	6.10	3.80	3.71
Pd(1)-S(1)	2.3980	2.3754	2.3786	2.3710	
Pd(1)-S(2)	2.3784	2.3579	2.3647	2.3531	
Pd(1)-P(1)	2.3674	2.3454	2.3561	2.3413	
Pd(1)-Cl(1)	2.3967	2.3747	2.3738	2.3700	
Ru(1)-N(1)	2.0547	2.0386	2.0461	2.0344	
Ru(1)-N(2)	2.0608	2.0451	2.0532	2.0411	
Ru(1)-Cl(2)	2.4399	2.4207	2.4252	2.4149	
S(1)-C(1)	1.7759	1.7592	1.7588	1.7580	
S(2)-C(2)	1.7839	1.7714	1.7717	1.7702	
N(1)-C(1)	1.3393	1.3219	1.3154	1.3215	
N(2)-C(2)	1.3360	1.3162	1.3096	1.3158	
C(1)-C(2)	1.4727	1.4753	1.4851	1.4750	
S(1)-Pd(1)-P(1)	177.46	177.27	177.31	177.16	
P(1)-Pd(1)-S(2)	92.72	92.14	91.97	92.16	
S(2)-Pd(1)-Cl(1	177.74	178.39	178.44	178.39	
P(1)-Pd(1)-Cl(1)	89.40	89.47	89.58	88.83	
N(2)-Ru(1)-N(1)	76.92	76.94	76.84	77.02	
N(2)-Ru(1)-Cl(2	85.77	85.35	85.65	85.32	
N(1)-Ru(1)-Cl(2)	85.12	85.90	86.28	85.81	

Compound C

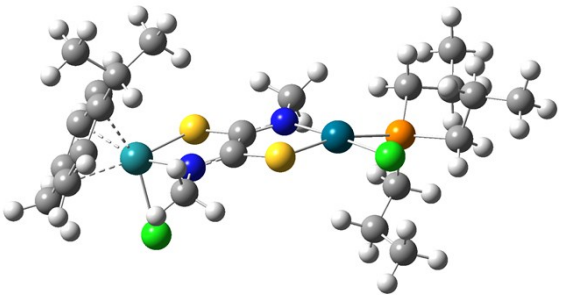

Functional	PSSTPSS	HSEH1PBE	CAMBLYP	PBE1PBE	ΔE(mean)
E(a.u.)	-3291.841298	-3289.699699	-3290.802477	-3289.539538	
ΔE(HOMO-LUMO)eV	1.88	3.00	6.09	3.81	3.69

Pd(1)-N(1)	2.0505	2.0529	2.0584	2.0456	
Pd(1)-P(1)	2.4346	2.4115	2.4037	2.3858	
Pd(1)-S(2)	2.3796	2.3525	2.3583	2.3549	
Pd(1)-Cl(1)	2.3835	2.3627	2.3629	2.3584	
Ru(1)-N(2)	2.0711	2.0609	2.0701	2.0563	
Ru(1)-S(1)	2.4207	2.3952	2.4090	2.3933	
Ru(1)-Cl(2)	2.4506	2.4278	2.4311	2.4210	
S(1)-C(1)	1.7879	1.7710	1.7622	1.7642	
S(2)-C(2)	1.7935	1.7748	1.7735	1.7734	
N(1)-C(1)	1.3397	1.3213	1.3178	1.3228	
N(2)-C(2)	1.3339	1.3158	1.3094	1.3153	
C(1)-C(2)	1.4747	1.4759	1.4844	1.4736	
N(1)-Pd(1)-P(1)	100.93	100.59	99.54	99.67	
N(1)-Pd(1)-S(2)	84.34	84.36	84.46	84.70	
P(1)-Pd(1)-S(2)	166.74	172.05	173.45	173.16	
N(1)-Pd(1)-Cl(1)	170.38	170.54	171.40	171.31	
P(1)-Pd(1)-Cl(1)	88.66	88.80	88.75	88.74	
S(2)-Pd(1)-Cl(1)	86.14	86.18	87.50	87.14	
N(2)-Ru(1)-S(1)	81.50	81.51	81.49	81.64	
N(2)-Ru(1)-Cl(2)	83.23	83.15	83.62	83.17	
S(1)-Ru(1)-Cl(2)	88.11	88.59	89.42	88.74	

Compound D

Functional	PSSTPSS	HSEH1PBE	CAMBLYP	PBE1PBE	RX	ΔE(mean)
E(a.u.)	-3291.857953	-3289.718251	-3290.817923	-3289.554956	-	
ΔE(HOMO-LUMO)eV	1.99	3.00	6.04	3.76	-	3.70
Pd(1)-N(1)	2.0725	2.0701	2.0765	2.0671	2.082(4)	
Pd(1)-P(1)	2.3594	2.3353	2.3445	2.3312	2.248(1)	
Pd(1)-S(2)	2.3679	2.3472	2.3485	2.3423	2.262(1)	
Pd(1)-Cl(1)	2.4158	2.3937	2.3937	2.3891	2.316(1)	
Ru(1)-N(2)	2.0719	2.0628	2.0731	2.0583	2.095(4)	
Ru(1)-S(1)	2.4227	2.3990	2.4072	2.3934	2.347(1)	
Ru(1)-Cl(2)	2.4493	2.4284	2.4327	2.4223	2.418(2)	
S(1)-C(1)	1.7879	1.7692	1.7668	1.7676	1.719(5)	
S(2)-C(2)	1.8015	1.7849	1.7838	1.7832	1.734(5)	
N(1)-C(1)	1.3332	1.3154	1.3105	1.3153	1.290(6)	
N(2)-C(2)	1.3295	1.3113	1.3051	1.3110	1.289(5)	
C(1)-C(2)	1.4752	1.4746	1.4857	1.4746	1.485(6)	
N(1)-Pd(1)-P(1)	178.80	178.61	178.24	178.57	177.05(11)	
N(1)-Pd(1)-S(2)	84.68	84.68	84.58	84.78	84.29(11)	
P(1)-Pd(1)-S(2)	94.48	94.43	94.11	94.32	93.13(5)	
N(1)-Pd(1)-Cl(1	96.58	93.81	96.86	96.83	94.48(11)	
P(1)-Pd(1)-Cl(1)	84.25	84.07	84.43	84.07	88.03(6)	
S(2)-Pd(1)-Cl(1)	178.63	178.49	178.44	178.34	177.00(7)	
N(2)-Ru(1)-S(1)	81.49	81.64	81.60	81.76	81.10(10)	
N(2)-Ru(1)-Cl(2	87.73	82.95	83.33	82.92	83.58(12)	
S(1)-Ru(1)-Cl(2)	89.27	89.52	90.07	89.41	87.96(5)	